

Supporting Information

Functional Layer-By-Layer Design of Xerogel-Based 1st Generation Amperometric Glucose Biosensors

Nicholas G. Poulos, Jackson R. Hall, and Michael C. Leopold*

Department of Chemistry, Gottwald Center for the Sciences, University of Richmond, Richmond, VA 23173

Contents:

- ▶ Amperometric I-t curves showing current response to interferent species injected at polyphenol membranes of different thickness (i.e., different electropolymerization times). *[Fig. SI-1]*

- ▶ Amperometric I-t curves and corresponding calibration curves for OTMS, HMTES, and IBTMS systems featuring only GOx-doped and undoped xerogel layers with and without polyphenol and polyurethane layers (i.e., Control experiments analogous to Figure 2). *[Figs. SI-2, SI-3, and SI-4]*

- ▶ Amperometric I-t curves during injection of common interferent species (acetaminophine, ascorbic acid, sodium nitrite, oxalic acid, uric acid) and target analyte (glucose) at OTMS, HMTES, and IBTMS xerogel sensing systems (i.e., interferent testing analogous to Figure 3A). *[Figs. SI-5, SI-7, and SI-9]*

- ▶ Selectivity coefficients of common interferent species (acetaminophine, ascorbic acid, sodium nitrite, oxalic acid, uric acid) and target analyte (glucose) at OTMS, HMTES, and IBTMS xerogel sensing systems (i.e., interferent testing analogous to Figure 3B). *[Figs. SI-6, SI-8, and SI-10]*

- ▶ Stability results (sensitivity and response time) for OTMS, HMTES, IBTMS, and MPTMS xerogel sensing systems (i.e., stability tests analogous to Figure 4). *[Figs. SI-11, SI-12, SI-13, SI-14]*

- ▶ Literature comparison of sensing performance attributes. *[Table SM-1]*

- ▶ Selectivity coefficient comparison. *[Table SM-2]*

- ▶ Scanning electron microscopy (SEM) imaging of various xerogel films. *[Fig. SI-15]*

- ▶ Cyclic voltammetry of HMFc redox probe at various xerogel films. *[Fig. SI-16]*

* To whom correspondence should be addressed. Email: mleopold@richmond.edu.
Phone: (804) 287-6329. Fax: (804) 287-1897.

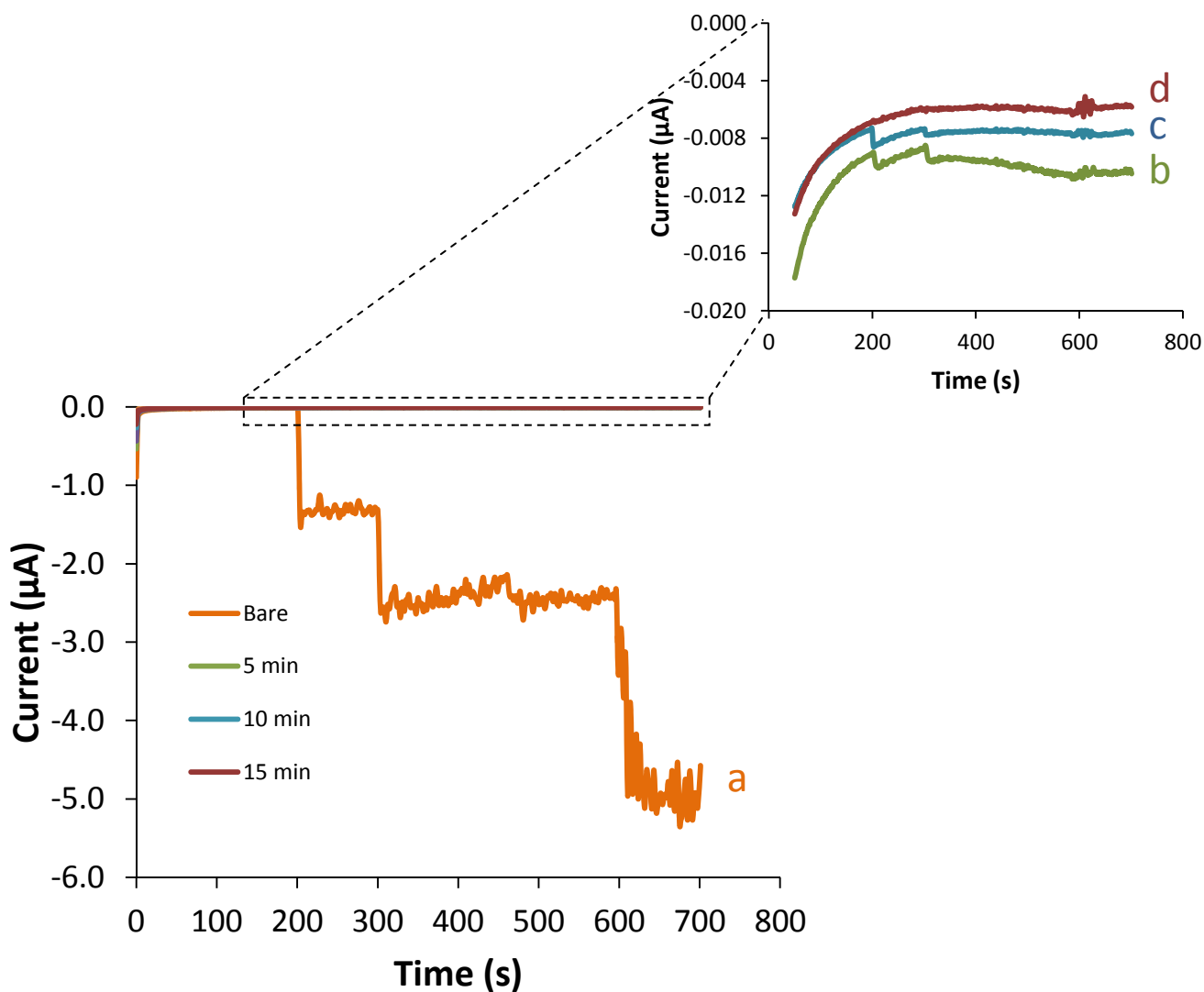


Figure SI-1. Amperometric I-t curves during successive injections of interferent species at (a) unmodified platinum electrodes and electrodes modified by electropolymerizing unstabilized phenol for (b) 5, (c) 10, and (d) 15 minutes. Each injection of interferent (acetaminophen at 200 sec.; ascorbic acid at 300 sec.; oxalic acid at 400 sec.; sodium nitrate at 500 sec.; uric acid at 600 sec.) resulted in a concentration of 100 μM in 25 mL of 4.4mM PBS (pH=7.00). NOTE: Data smoothed for visual purposes (Least square smoothing).

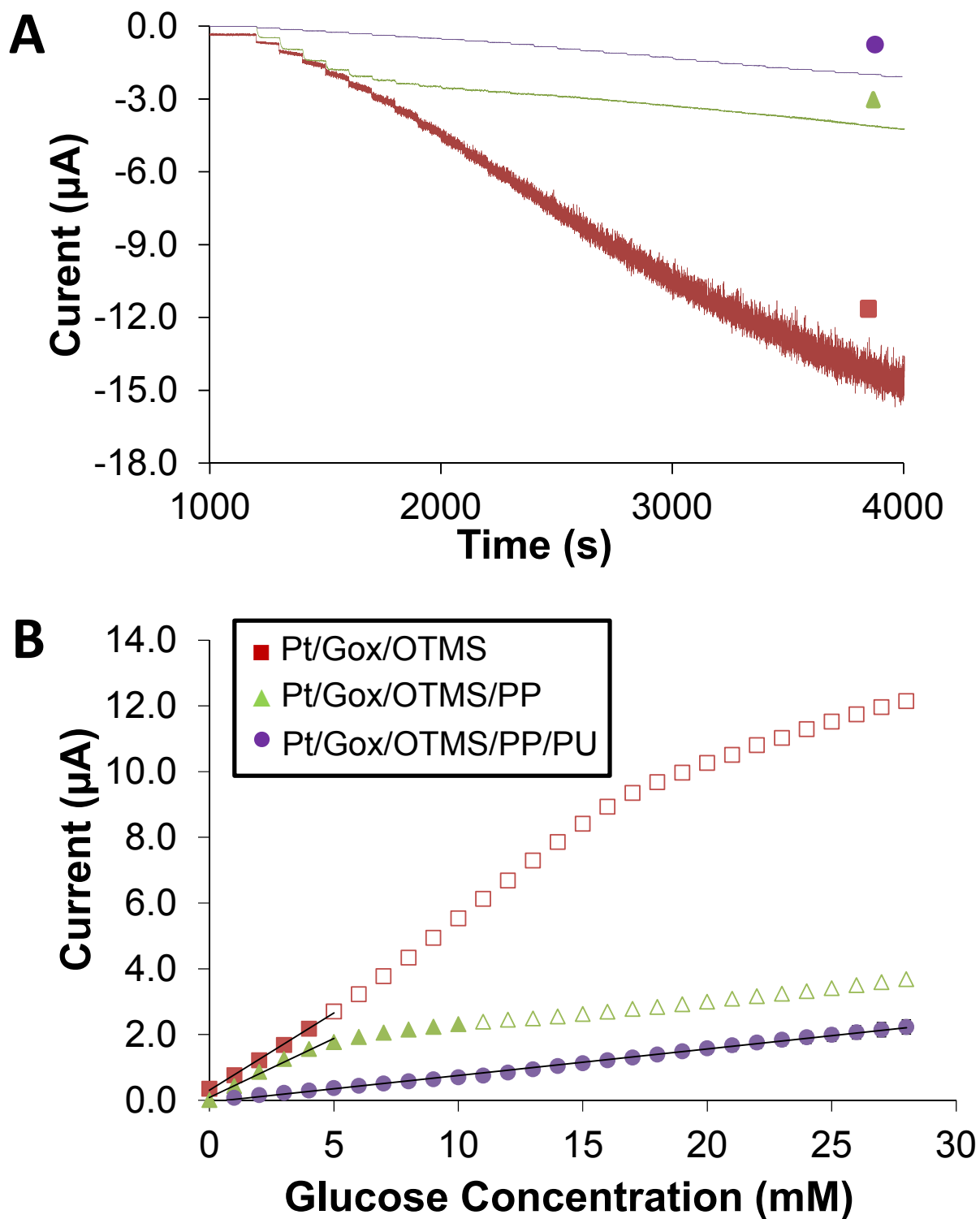


Figure SI-2. (A) Amperometric $I-t$ curve and (B) corresponding calibration curves during successive 1 mM injections of glucose at a platinum electrode modified with GOx-doped OTMS xerogel, un-doped OTMS xerogel, poly-phenol (PP), and polyurethane layers (PU) at the various stages of L-B-L construction of the xerogel-based sensor. Solid symbols indicate a step like response whereas open symbols indicate a non-step response (dynamic range). Linear regression is performed for linear step-responses (linear range).

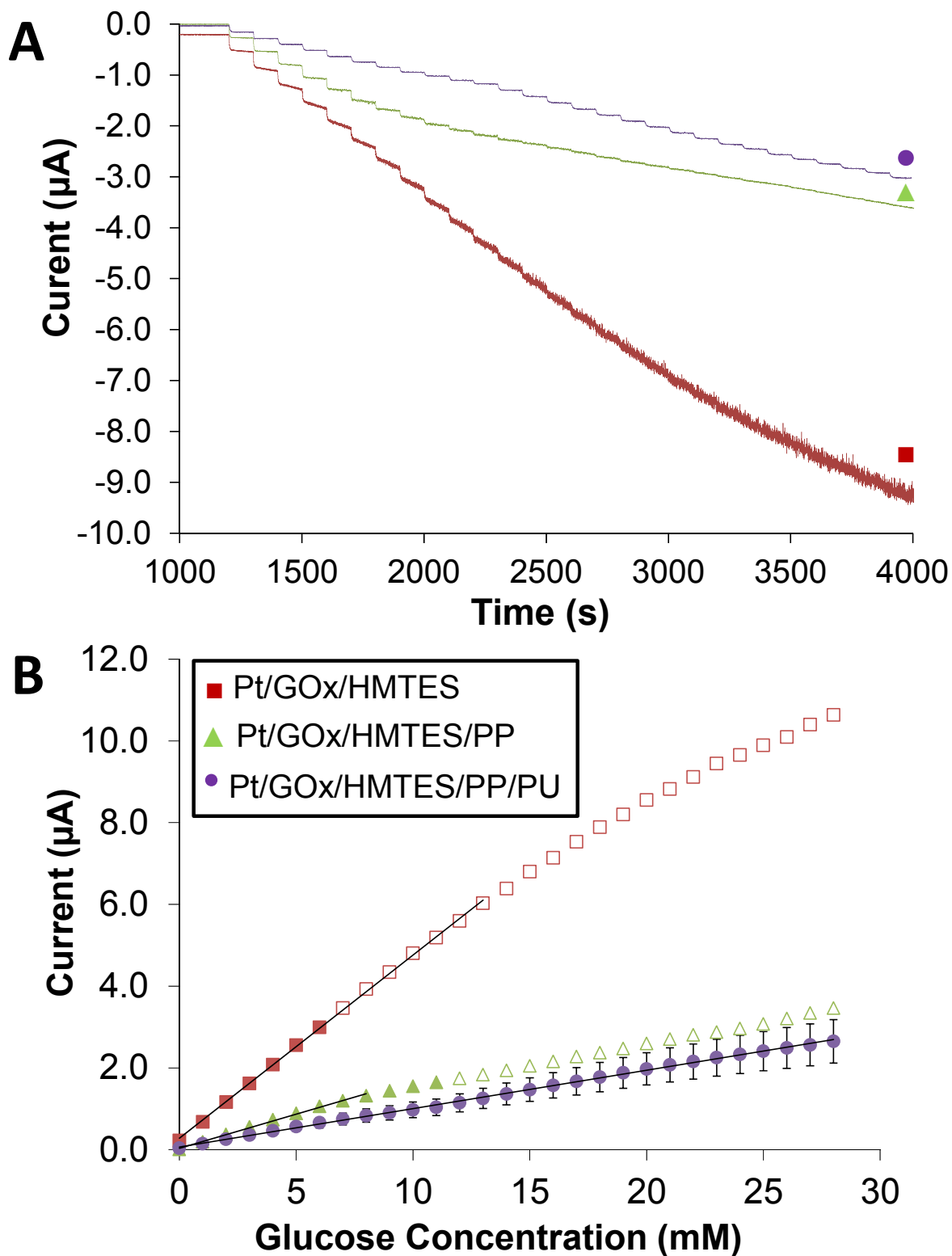


Figure SI-3. (A) Amperometric $I-t$ curve and (B) corresponding calibration curves during successive 1 mM injections of glucose at a platinum electrode modified with GOx-doped **HMTES** xerogel, un-doped **HMTES** xerogel, poly-phenol (PP), and polyurethane layers (PU) at the various stages of L-B-L construction of the xerogel-based sensor. Solid symbols indicate a step like response whereas open symbols indicate a non-step response (dynamic range). Linear regression is performed for linear step-responses (linear range).

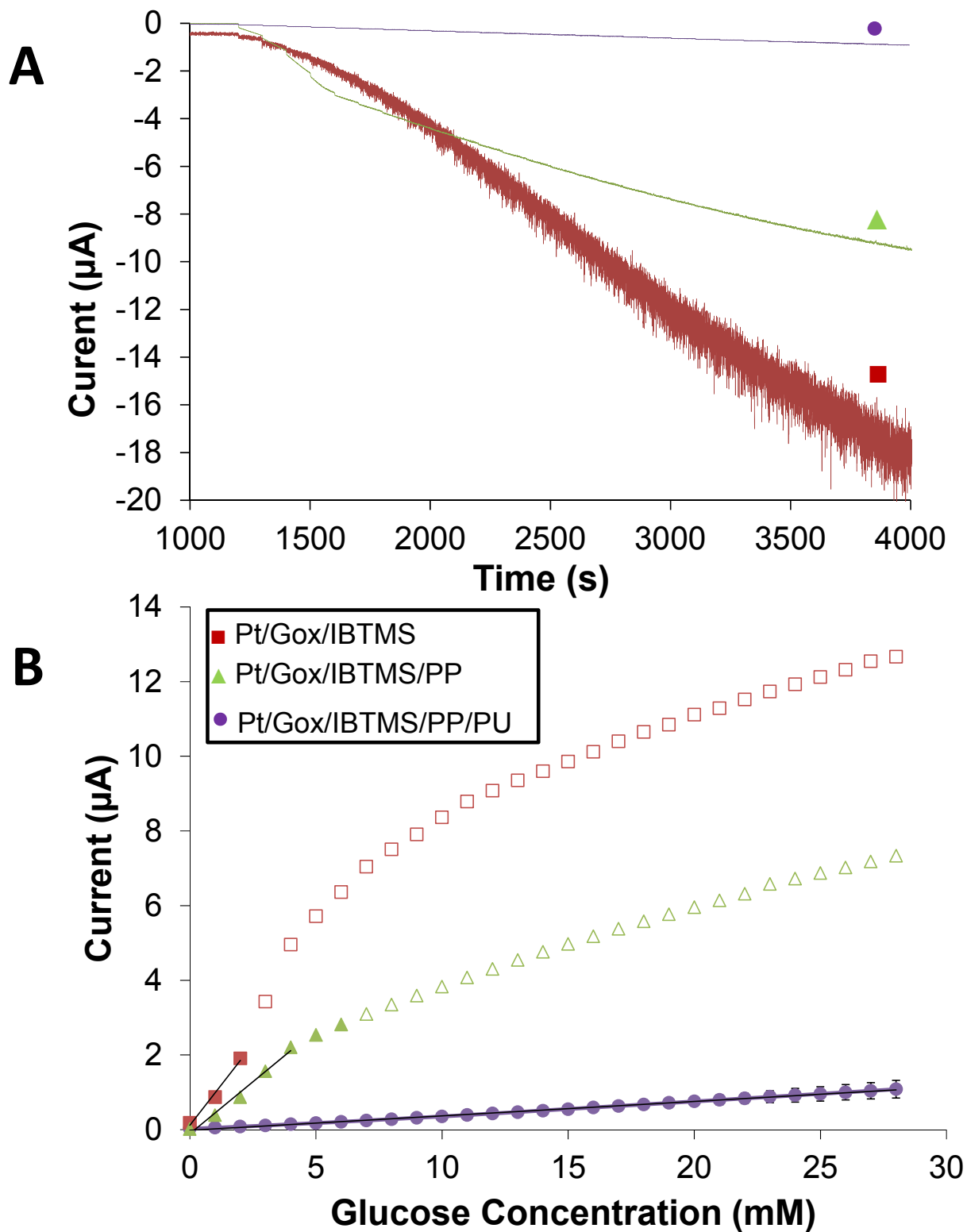


Figure SI-4. (A) Amperometric $I-t$ curve and (B) corresponding calibration curves during successive 1 mM injections of glucose at a platinum electrode modified with GOx-doped IBTMS xerogel, undoped IBTMS xerogel, poly-phenol (PP), and polyurethane layers (PU) at the various stages of L-B-L construction of the xerogel-based sensor. Solid symbols indicate a step like response whereas open symbols indicate a non-step response (dynamic range). Linear regression is performed for linear step-responses (linear range).

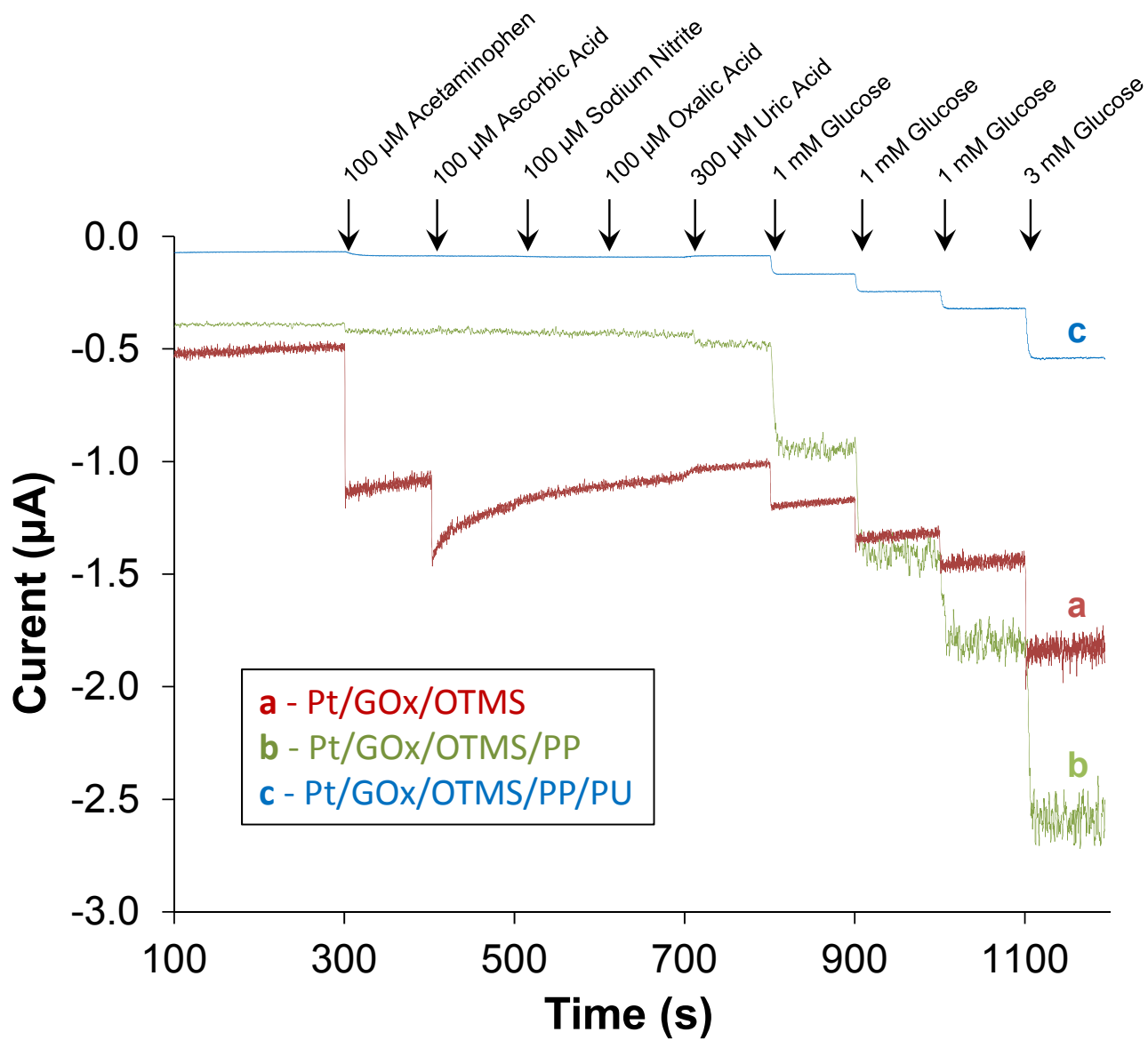


Figure SI-5. Amperometric *I-t* curve successive injections of common interferent species (100 µM) and glucose (1 mM or 3 mM) at a platinum electrode modified with various stages of L-B-L construction including (a) GOx-doped OTMS xerogel and un-doped OTMS xerogel with (b) poly-phenol (PP) or with (c) poly-phenol and polyurethane (PU) capping layers. Note: The interferent uric acid was tested at 300 µM.

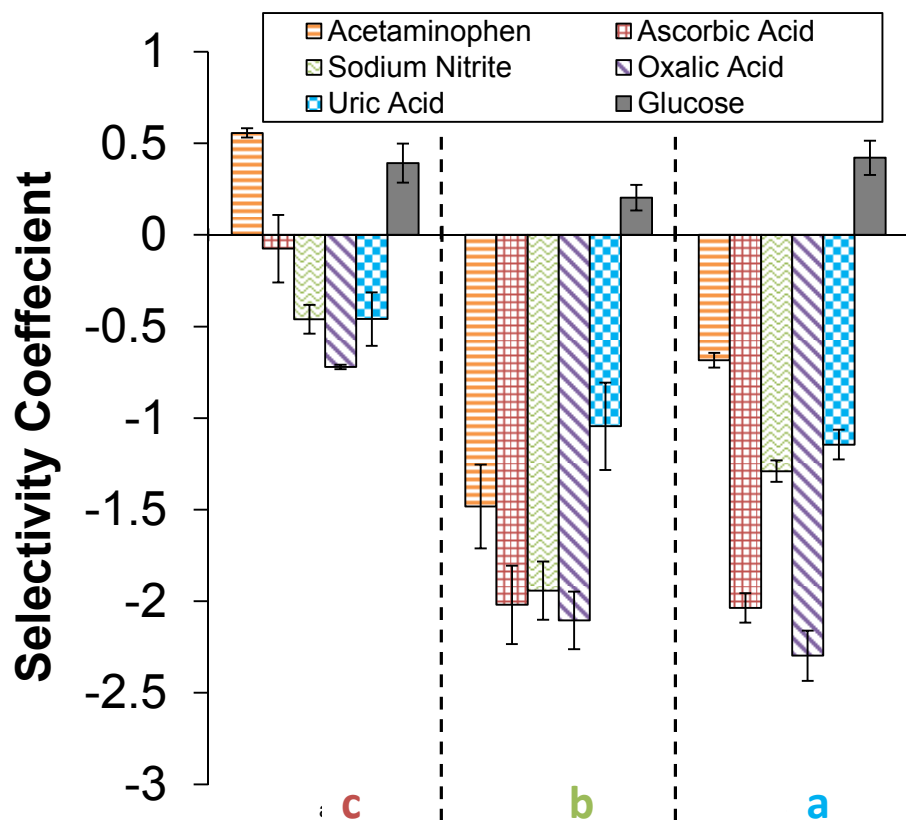


Figure SI-6. Selectivity coefficient tracking during successive injections of common interferent species (100 μM) and glucose (3 mM) at a platinum electrode modified with various stages of L-B-L construction including (a) GOx-doped OTMS xerogel and un-doped OTMS xerogel with (b) poly-phenol (PP) or with (c) poly-phenol and polyurethane (PU) capping layers. Note: The interferent uric acid was tested at 300 μM .

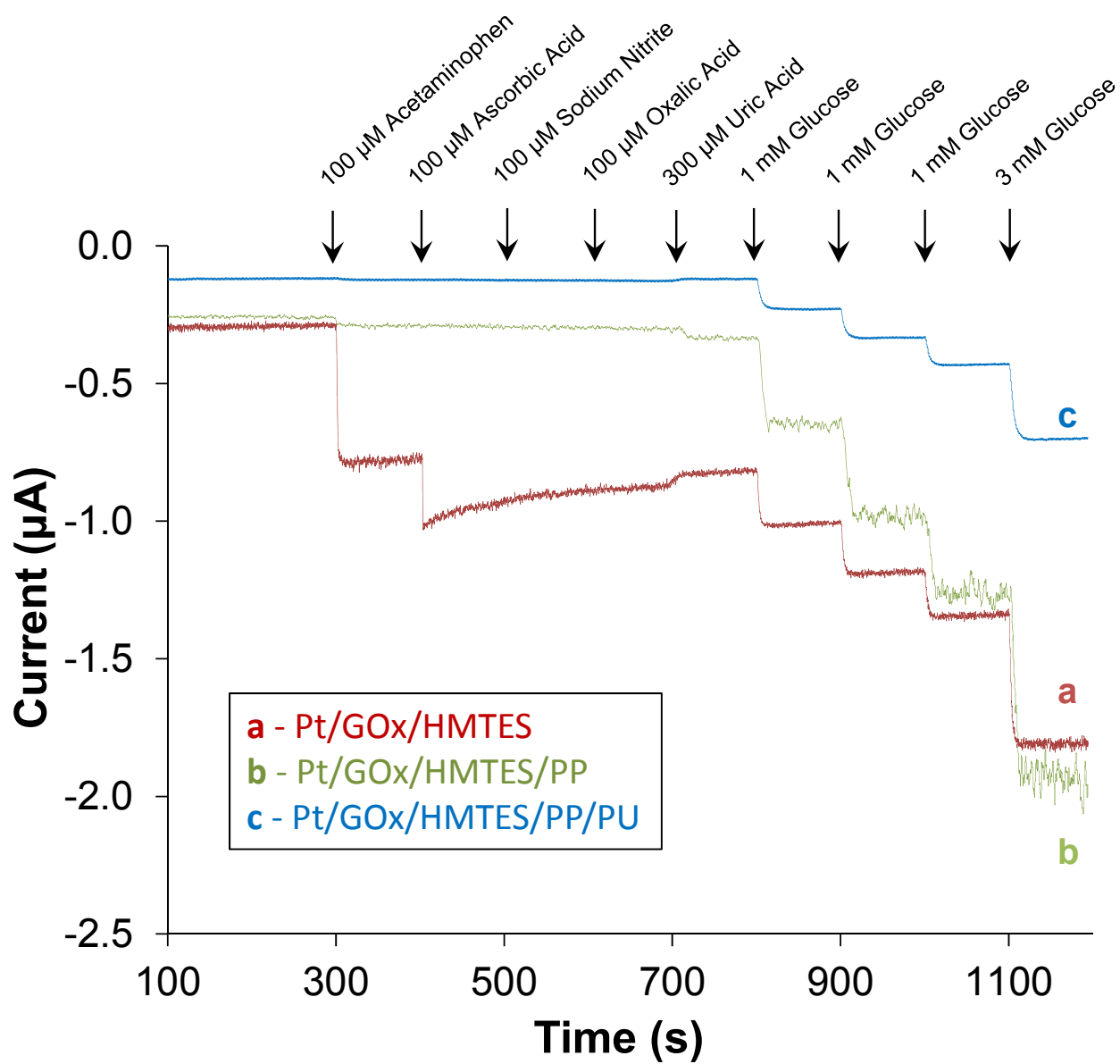


Figure SI-7. Amperometric $I-t$ curve successive injections of common interferent species (100 μM) and glucose (1 mM or 3 mM) at a platinum electrode modified with various stages of L-B-L construction including (a) GOx-doped HMTES xerogel and un-doped HMTES xerogel with (b) poly-phenol (PP) or with (c) poly-phenol and polyurethane (PU) capping layers. Note: The interferent uric acid was tested at 300 μM .

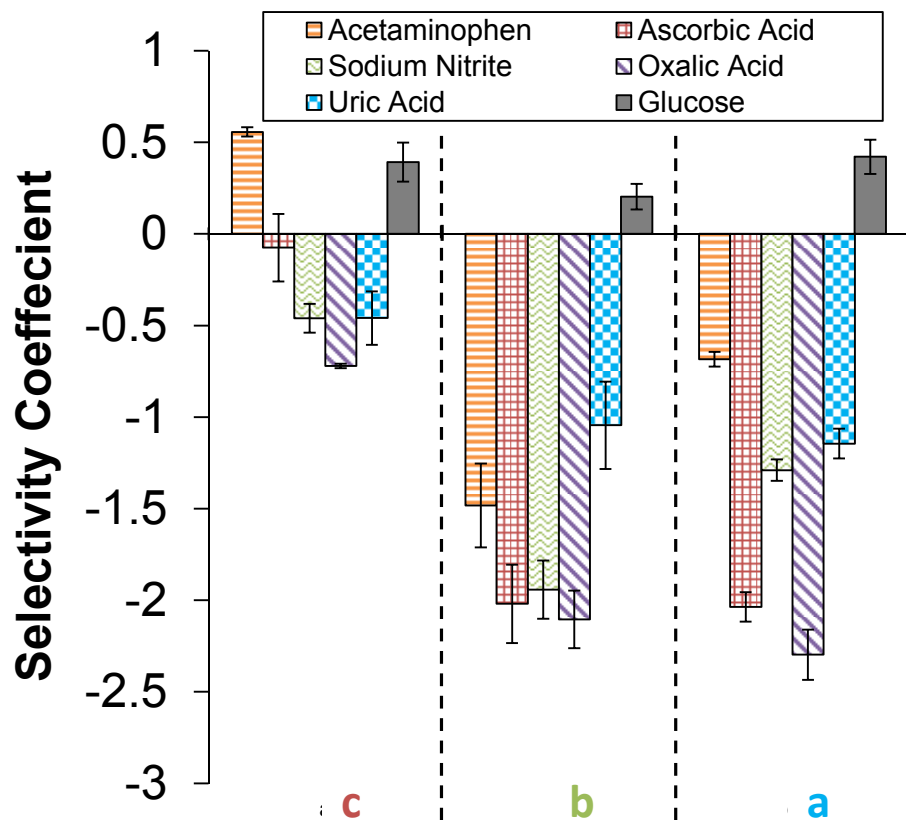


Figure SI-8. Selectivity coefficient tracking during successive injections of common interferent species (100 μM) and glucose (1 mM or 3 mM) at a platinum electrode modified with various stages of L-B-L construction including (a) GOx-doped **HMTES xerogel** and un-doped HMTES xerogel with (b) poly-phenol (PP) or with (c) poly-phenol and polyurethane (PU) capping layers. Note: The interferent uric acid was tested at 300 μM .

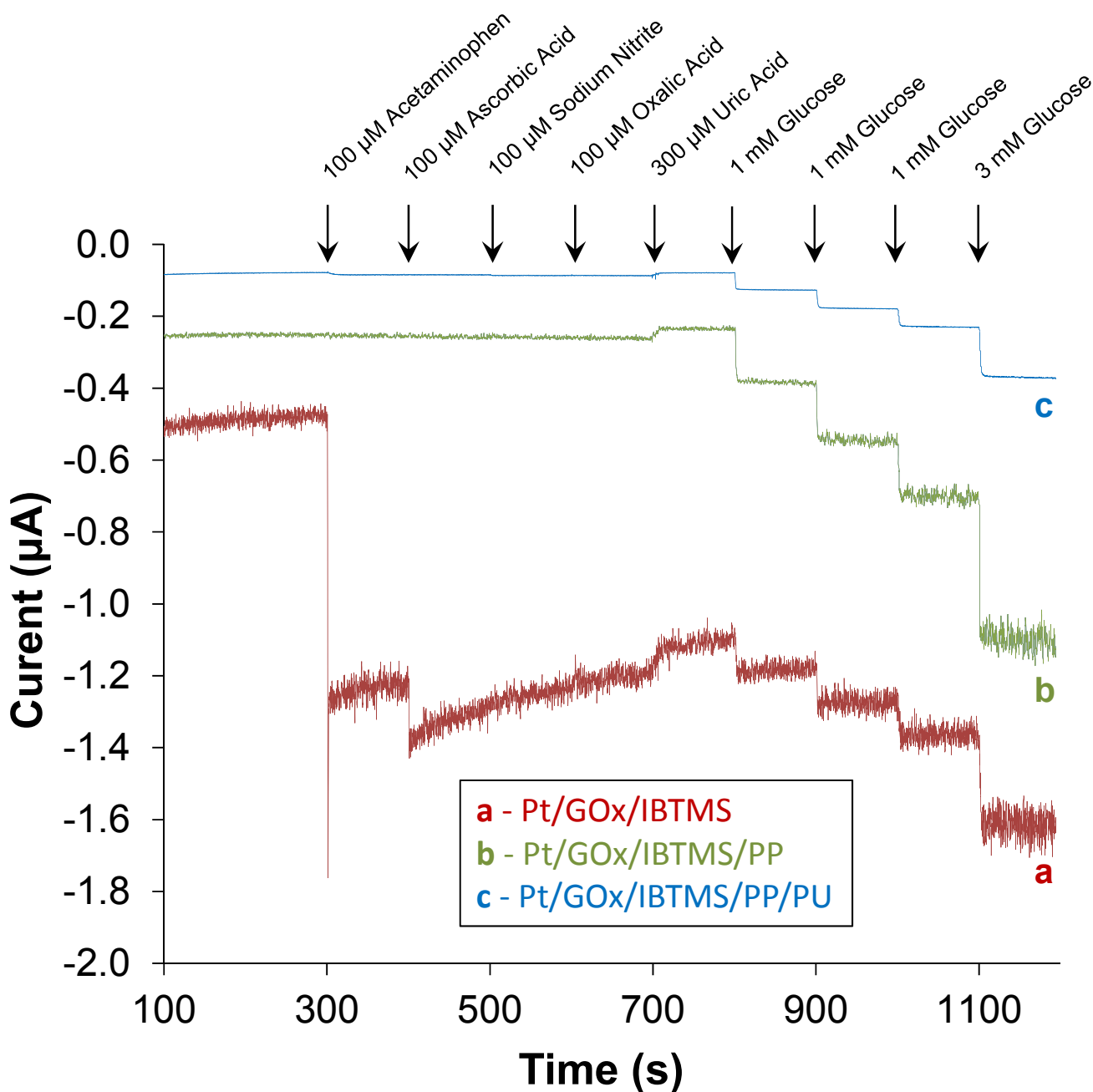


Figure SI-9. Amperometric *I-t* curve successive injections of common interferent species (100 μM) and glucose (1 mM or 3 mM) at a platinum electrode modified with various stages of L-B-L construction including (a) GOx-doped IBTMS xerogel and un-doped IBTMS xerogel with (b) poly-phenol (PP) or with (c) poly-phenol and polyurethane (PU) capping layers. Note: The interferent uric acid was tested at 300 μM .

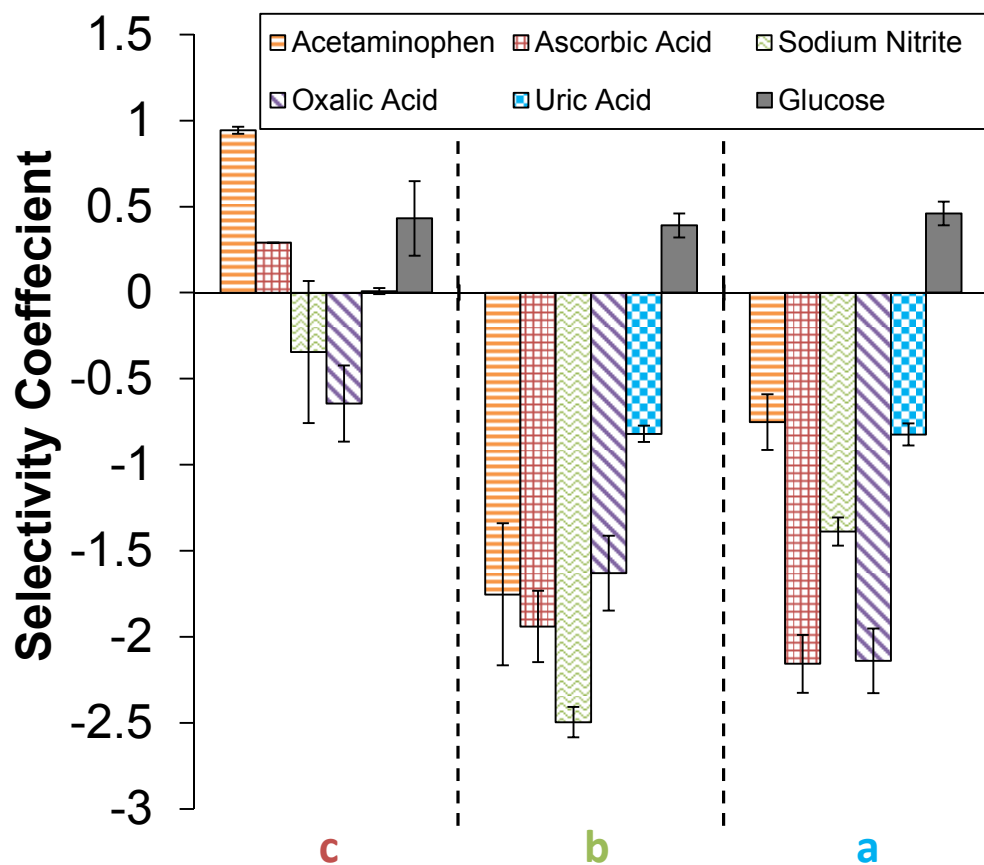


Figure SI-10. Selectivity coefficient tracking during successive injections of common interferent species (100 μM) and glucose (1 mM or 3 mM) at a platinum electrode modified with various stages of L-B-L construction including (a) GOx-doped **IBTMS xerogel** and un-doped IBTMS xerogel with (b) poly-phenol (PP) or with (c) poly-phenol and polyurethane (PU) capping layers. Note: The interferent uric acid was tested at 300 μM .

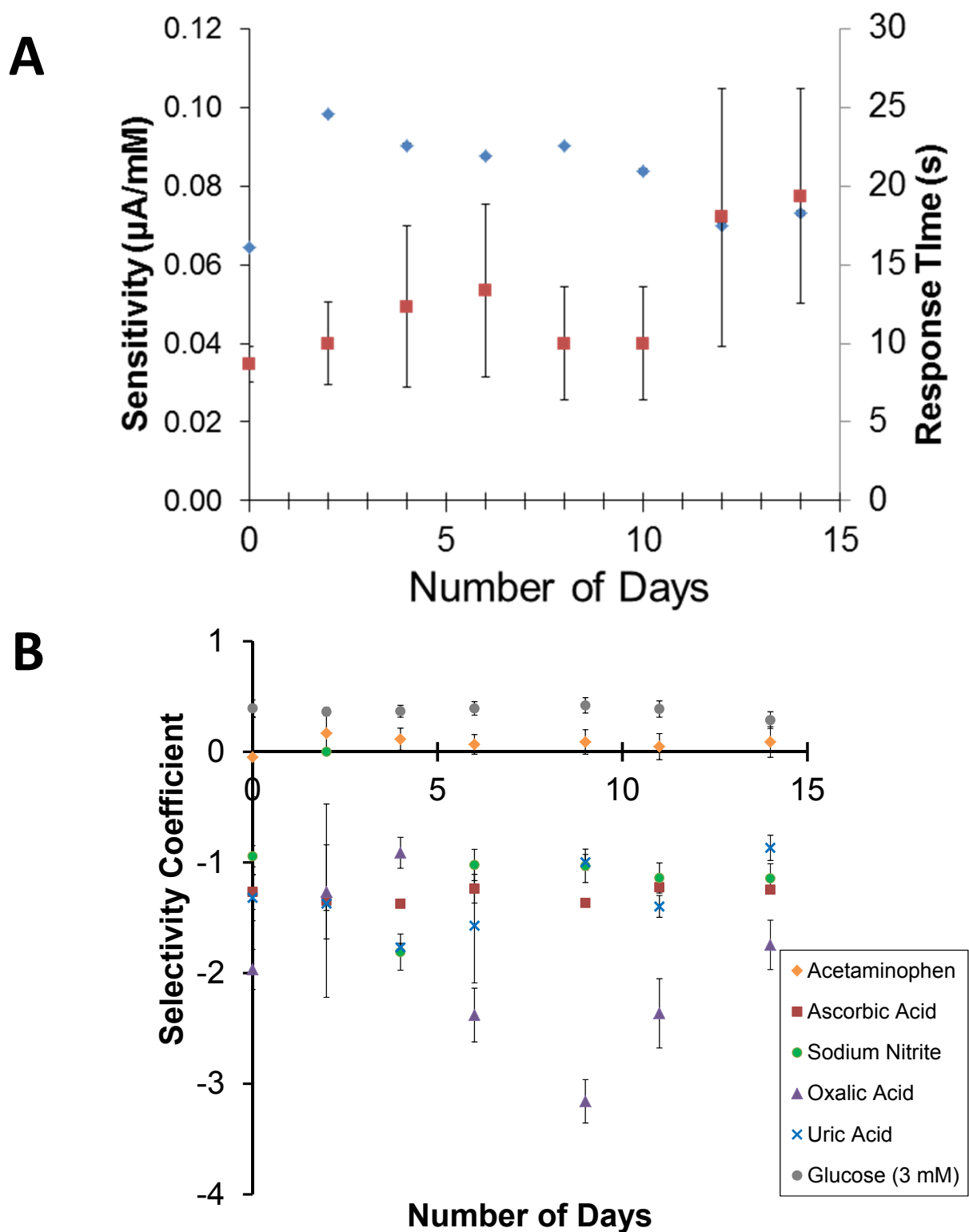


Figure SI-11. (A) Stability tests for layered OTMS xerogel glucose biosensors with sensitivity (\blacklozenge) and response time (\blacksquare) as well as (B) the selectivity coefficients of common interferents and glucose (3 mM) monitored over a two week period. Sensors were stored at 4-7°C immersed in PBS (pH 7; 4.4 mM) Note: In some cases, error bars are smaller than markers for average sensitivity.

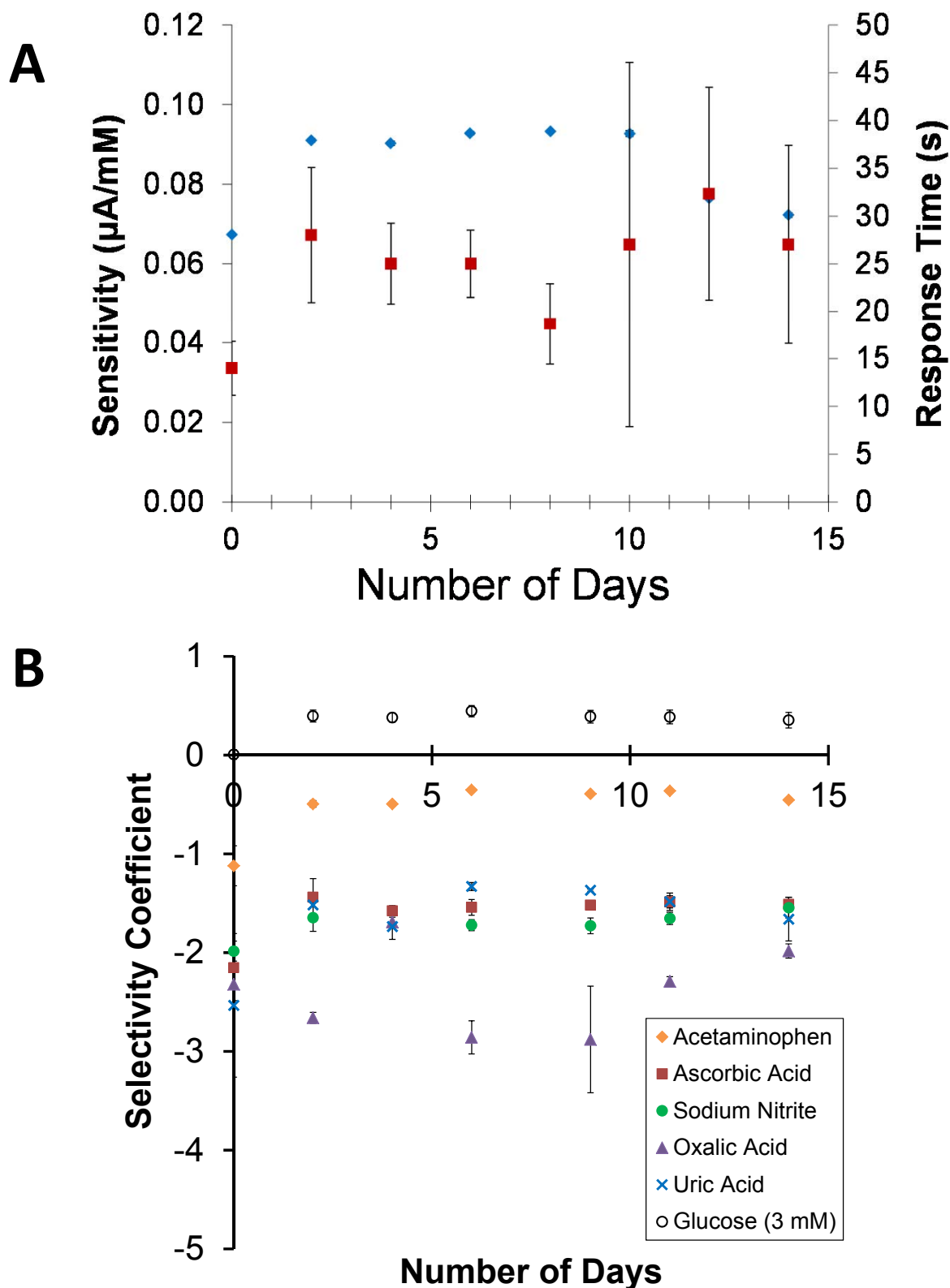


Figure SI-12. (A) Stability tests for layered HMTES xerogel glucose biosensors with sensitivity (\blacklozenge) and response time (\blacksquare) as well as (B) the selectivity coefficients of common interferents and glucose (3 mM) monitored over a two week period. Sensors were stored at 4-7°C immersed in PBS (pH 7; 4.4 mM) Note: In some cases, error bars are smaller than markers for average sensitivity.

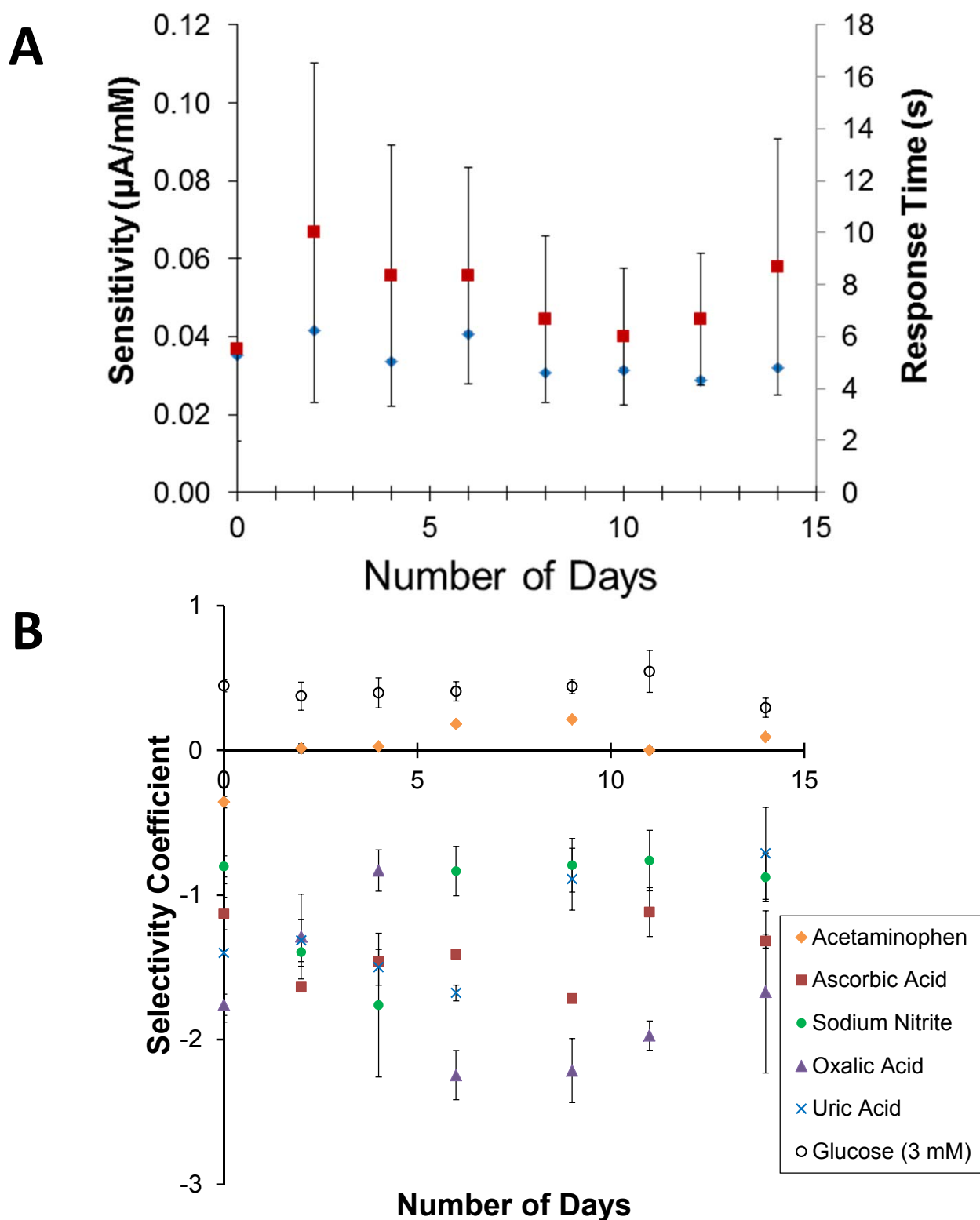


Figure SI-13. (A) Stability tests for layered **IBTMS xerogel** glucose biosensors with sensitivity (\blacklozenge) and response time (\blacksquare) as well as (B) the selectivity coefficients of common interferents and glucose (3 mM) monitored over a two week period. Sensors were stored at 4-7°C immersed in PBS (pH 7; 4.4 mM) Note: In some cases, error bars are smaller than markers for average sensitivity.

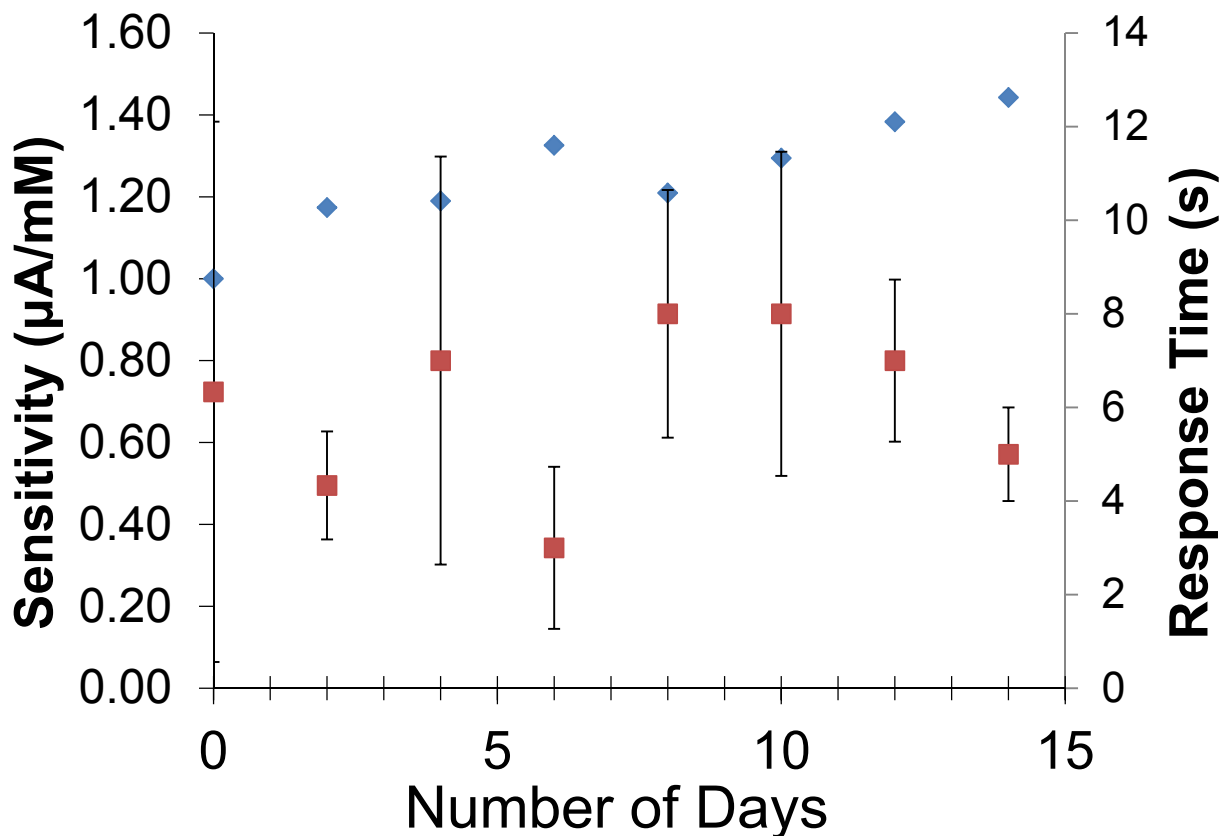


Figure SI-14. Stability tests for layered 3-MPTMS xerogel glucose biosensors monitored over two weeks for sensitivity (♦) and response time (■). Sensors were stored at 4-7°C immersed in PBS (pH 7; 4.4 mM). Note: In some cases, error bars are smaller than markers for average sensitivity

Table SM-1: Comparison of 1st Generation Amperometric Glucose Biosensor Performance Parameters – Literature Comparison

System	WE	Sensitivity ($\mu\text{A}/\text{mM}$)	Response Time (s)	Linear Range ^a (mM)	Dynamic Range ^a (mM)	LOD (μM) ^b	Stability	Ref ^c
PTMS	Pt	0.0983 (± 0.0007)	16.5 (± 9.3)	>28	>28	18.1 (± 2.2)	>2 wk.	<i>d</i>
OTMS	Pt	0.1671 (± 0.0014)	17.5 (± 2.1)	21	28	18.8 (± 0.02)	>2 wk.	<i>d</i>
HMTES	Pt	0.1141 (± 0.0010)	27.0 (± 2.8)	24	28	8.2 (± 3.5)	>2 wk.	<i>d</i>
IBTMS	Pt	0.0939 (± 0.0009)	20.5 (± 12.0)	25	28	21.5 (± 6.2)	>2 wk.	<i>d</i>
Selected Sol-gel Based Glucose Sensors								
MPTMS	Pt	0.072 _(.002)	45.5 _(25.9)	7	12	30.7 _(20.4)	>2 wk.	<i>1</i>
MPTMS	Pt	0.0035	11-12	12.5	20	-	5 mo.	<i>2</i>
TEOS	ITO	-	<30	15	30	-	2 mo.	<i>3</i>
MTMS	Pt	0.038	20-65	20-30	-	-	2 wk.	<i>4</i>
MTMS	Pt	0.11	28.2	-	6	-	-	<i>5</i>
MPTMS/TEOS	GCE	0.81	15 (90%)	4.4	-	19	3 wk.	<i>6</i>
Nafion (Wire)	Pt	0.0022	60	9	20	-	2 wk.	<i>7</i>
Selected Glucose Sensors (with Nanoparticle Doping)								
MPTMS with MPCs	Pt	0.184 _(0.005)	11.3 _(6.6)	14	22	23.2 _(5.5)	>2 wk.	<i>1</i>
MPTMS sol-gel/CSNPs	Au	0.26	3	6	-	23	2 mo.	<i>8</i>
Cysteamine films/CSNPs	Au	0.18	4	8	-	8	4 wk.	<i>9</i>
CSNPs/ CNT	Au	0.23	-	9	-	128	3 wk.	<i>10</i>
PVC/TTF-TCNQ	-	4.5E4	-	2	-	6.2	-	<i>11</i>
CSNPs & Silica NPs	Pt	-	60	<10	30	-	-	<i>12</i>
nanoPani	Pt	12.21 _(0.58)	3	0.01-5.5	-	0.3 _(0.1)	-	<i>13</i>
DMSA	Au	1.23	5	0.0008-4	-	0.3	-	<i>14</i>

a. Upper limit of range listed; **b.** Limit of Detection (L.O.D.) is the concentration required to elicit a sensor response ($3\sigma_{\text{BL}}$); **c.** References listed below; **d.** Current work

Notes: CS-NPs: Citrate-stabilized colloidal gold nanoparticles; MPTMS: 3-mercaptopropyltrimethoxy silane; MTMOS: methyltrimethoxy silane; TEOS: tetraethoxy silane; TMOS: tetramethoxy silane; APTEOS: 3-aminopropyltriethoxy silane; CNTs: carbon nanotubes; GrP: Graphite powder; DMSA: dimercaptosuccinic acid.

References – Table SM-1

- Freeman, M.; Hall, J.; Leopold, M.; *Analytical Chemistry*. **2013**, 85(8), 4057-4065
- Yang, Y.; Tseng, T.; Yeh, J.; Chen, C.; Lou, S. *Sensors and Actuators B*. **2008**, 131, 533-540.
- Narang, U.; Prasad, P. N.; Bright, F. V. *Anal. Chem.* **1994**, 66, 3139-3144.
- Shin, J. H.; Marxer, S. M.; Schoenfish, M. H. *Anal. Chem.* **2004**, 76, 4543-4549.
- Koh, A.; Riccio, D. A.; Sun, B.; Carpenter, A. W.; Nichols, S. P.; Schoenfish, M. H. *Biosens. and Bioelectron.* **2011**, 28, 17-24.
- Liu, S.; Sun, Y. *Biosensors and Bioelectronics*. **2007**, 22, 905-911.
- Ward, W. K.; Jansen, L. B.; Anderson, E.; Reach, G.; Klein, J. C.; Wilson, G. S. *Biosensors and Bioelectronics*. **2002**, 17, 181-189.
- Zhang, S.; Wang, N.; Niu, Y.; Sun, C. *Sensors and Actuators B*. **2005**, 109, 367-374.
- Yang, W.; Wang, J.; Zhao, S.; Sun, Y.; Sun, C. *Electrochem. Commun.* **2006**, 8, 665-672.
- Liu, Y.; Wu, S.; Ju, H.; Xu, L. *Electroanalysis*. **2007**, 19, 986-992.
- Sánchez-Obrero, G.; Cano, M.; Ávila, J.; Mayén, M.; Mena, M.; Pingarrón, J.; Rodríguez-Amaro, R. *Journal of Electroanalytical Chemistry*. **2009**, 634, 59-63.
- Tang, F.; Meng, X.; Chen, D.; Ran, J.; Zheng, C. *Science in China, Series B: Chemistry*. **2000**, 43, 268-274.
- Wang, Z.; Liu, S.; Wu, P.; Cai, C. *Analytical Chemistry* **2009**, 81, 1638-1645
- Wang, Z.; Luo, X.; Wan, Q.; Wu, K.; Yang, N. A. *Applied Materials & Interfaces* **2014**, 6, 17296-17305.

Table SM-2. Selectivity Coefficients (K_{amp}) For Common Interferents and Glucose (3 mM) at Various Layered Xerogel Biosensors

Xerogel Silane Precursor	n	I_{lim} with 1 mM Glucose [†] (μA)	Glucose (3 mM)	Pt/Xerogel + Enzyme/Xerogel/PP/PU				
				Acetaminophen (100 μM)	Ascorbic Acid (100 μM)	Sodium Nitrate (100 μM)	Oxalic Acid (100 μM)	Uric Acid (300 μM)
PTMS	3	0.2846 (± 0.0451)	0.0850 (± 0.0214)	-0.9073 (± 0.1018)	-1.911 (± 0.059)	-2.760 (± 0.189)	-2.181 (± 0.140)	-1.858 (± 0.168)
OTMS	3	0.0838 (± 0.0218)	0.4208 (± 0.0942)	-0.6845 (± 0.0405)	-2.036 (± 0.080)	-1.289 (± 0.058)	-2.296 (± 0.137)	-1.144 (± 0.081)
HMTES	3	0.1104 (± 0.0358)	0.3916 (± 0.1408)	-1.146 (± 0.2487)	-2.265 (± 0.663)	-1.943 (± 0.458)	-1.974 (± 0.145)	-1.168 (± 0.129)
IBTMS	3	0.0542 (± 0.0105)	0.1617 (± 0.0684)	-0.7523 (± 0.1617)	-2.156 (± 0.168)	-1.388 (± 0.081)	-2.139 (± 0.188)	-0.8242 (± 0.064)
Pt/Xerogel + Enzyme/Xerogel/PP								
PTMS	3	0.5890 (± 0.0559)	-0.2638 (± 0.0250)	-1.325 (± 0.0731)	-3.369 (± 0.255)	-2.750 (± 0.123)	-3.576 (± 0.464)	-1.702 (± 0.230)
OTMS	3	0.4007 (± 0.1298)	0.2027 (± 0.070)	-1.481 (± 0.229)	-2.019 (± 0.214)	-1.941 (± 0.159)	-2.104 (± 0.157)	-1.044 (± 0.238)
HMTES	3	0.1364 (± 0.1327)	0.5029 (± 0.4181)	-0.9027 (± 0.4759)	-1.473 (± 0.063)	-1.514 (± 0.122)	-1.608 (± 0.044)	-0.8800 (± 0.4749)
IBTMS	3	0.1683 (± 0.0163)	0.3905 (± 0.0694)	-1.754 (± 0.413)	-1.941 (± 0.207)	-2.496 (± 0.088)	-1.630 (± 0.217)	-0.8204 (± 0.0478)
Pt/Xerogel + Enzyme/Xerogel								
PTMS	3	1.106 (± 0.348)	-0.4274 (± 0.2160)	-0.1910 (± 0.0843)	-0.6760 (± 0.1221)	-1.363 (± 0.196)	-1.783 (± 0.045)	-0.4335 (± 0.0427)
OTMS	3	0.1364 (± 0.1328)	0.3708 (± 0.4181)	0.1183 (± 0.4759)	-1.473 (± 0.063)	-1.514 (± 0.122)	-1.607 (± 0.044)	-0.8800 (± 0.4748)
HMTES	3	0.2451 (± 0.1004)	0.3878 (± 0.1417)	0.3928 (± 0.1409)	0.1075 (± 0.1036)	-0.6499 (± 0.4904)	-0.9458 (± 0.5254)	-0.7290 (± 0.0558)
IBTMS	3	0.0896 (± 0.0287)	0.4315 (± 0.2160)	0.9438 (± 0.0200)	0.2905 (± 0.0008)	-0.3450 (± 0.4128)	-0.6442 (± 0.2216)	0.0086 (± 0.0178)

Notes: [†] Steady-state limited amperometric current after injection of 1 mM glucose.

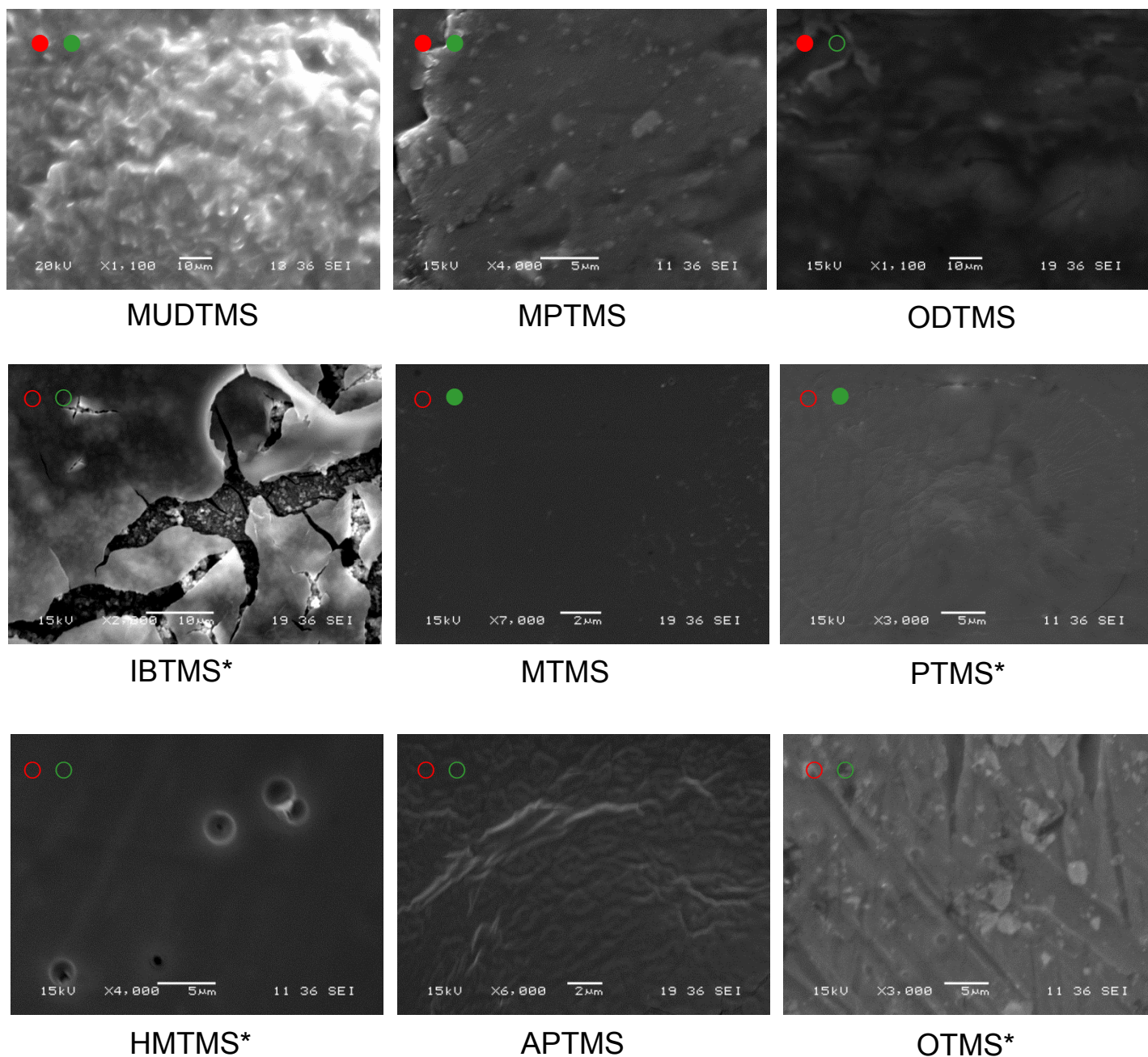


Figure SI-15. Representative scanning electron microscopy imaging of xerogel films formed from various silane precursors (see images). Note: Images are arranged (*left to right*) in same order as Table 2 (i.e., least permeable/porous to most permeable/porous). Red and green *open* symbols signify any significant diffusional redox probe behavior observed for anionic/cationic ferricyanide/ruthenium hexamine (○) (which behaved similarly in all cases) and HMFc (○), respectively. Non-diffusional (blocked) behaviors are correspondingly marked with *closed* symbols (●, ●). Systems marked with (*) were the most successful xerogels in terms of glucose biosensing response schemes (i.e., capped with poly-phenol and polyurethane layers).

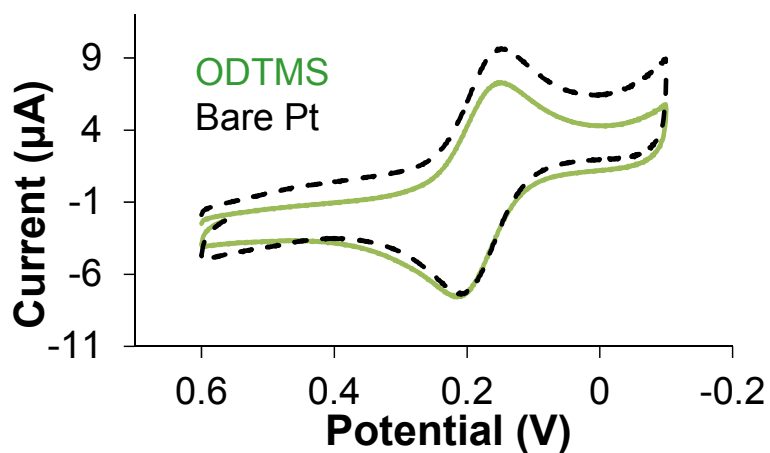
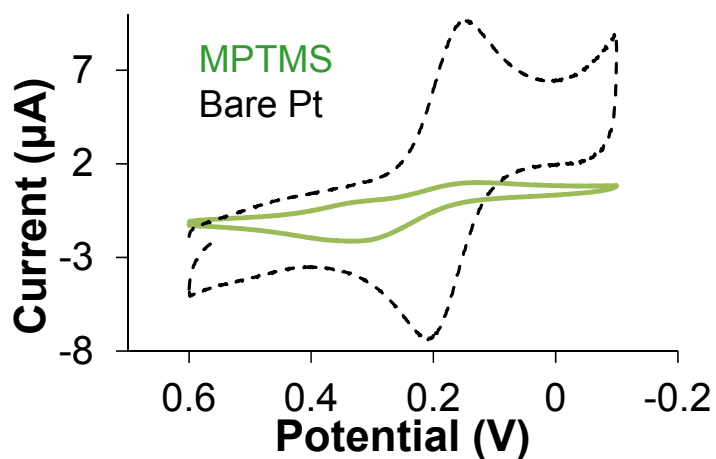
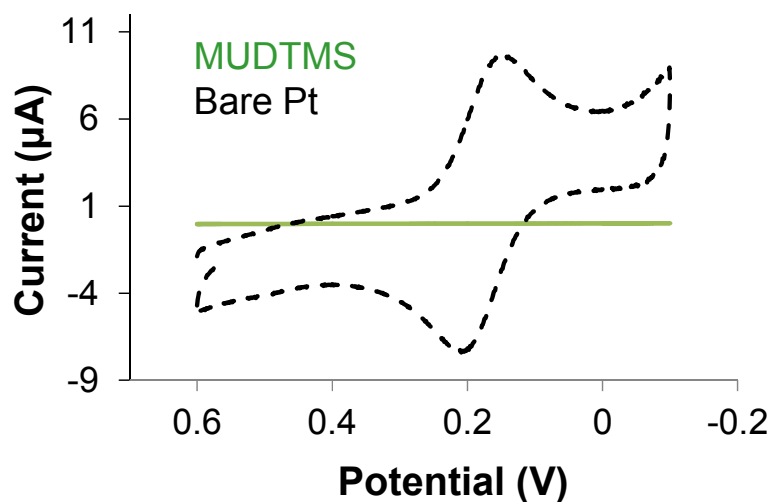


Figure SI-16. Cyclic voltammetry of neutral 1 mM HMFc in in 0.1 M HClO_4 at platinum electrodes modified with xerogels formed from different silanes (green; solid trace) versus at a bare platinum electrode (black; dashed) including **MUDTMS**, **MPTMS**, and **ODTMS**. HMFc voltammetry was recorded at 25 mV/sec. Note: *Systems exhibiting the best glucose sensing responses.

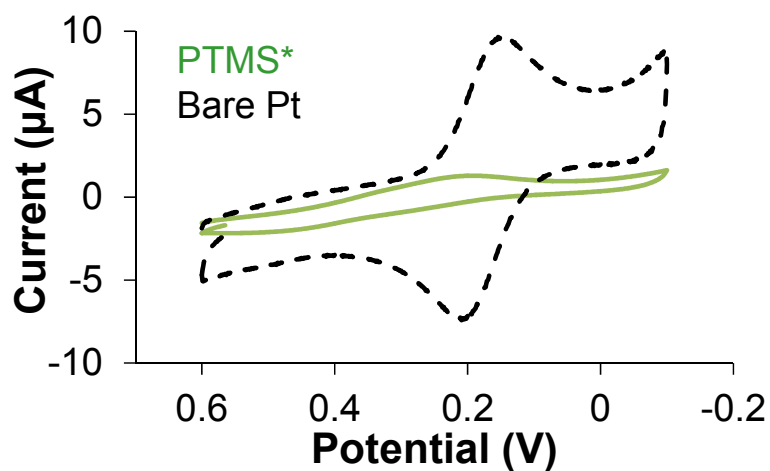
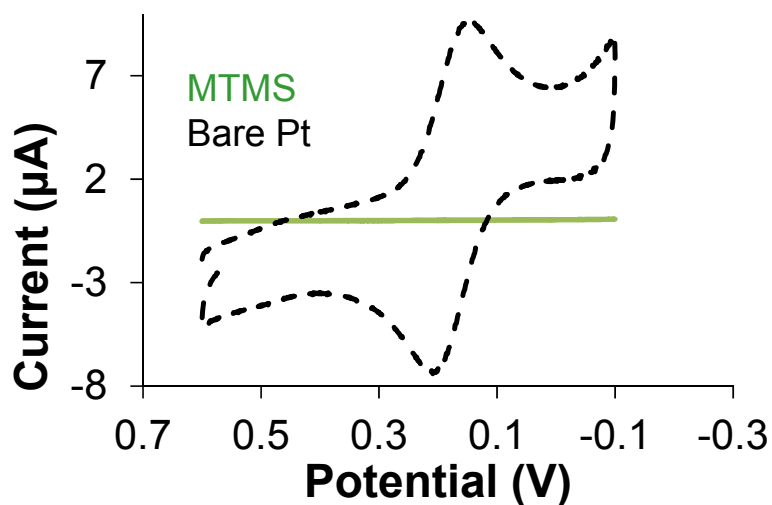
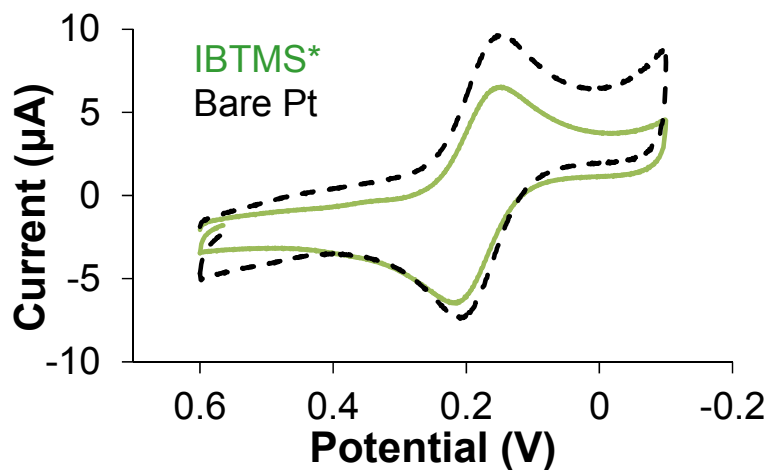


Figure SI-16. Cyclic voltammetry of neutral 1 mM HMFC in in 0.1 M HClO_4 at platinum electrodes modified with xerogels formed from different silanes (green; solid trace) versus at a bare platinum electrode (black; dashed) including **IBTMS**, **MTMS**, and **PTMS**. HMFC voltammetry was recorded at 25 mV/sec. Note: *Systems exhibiting the best glucose sensing responses.

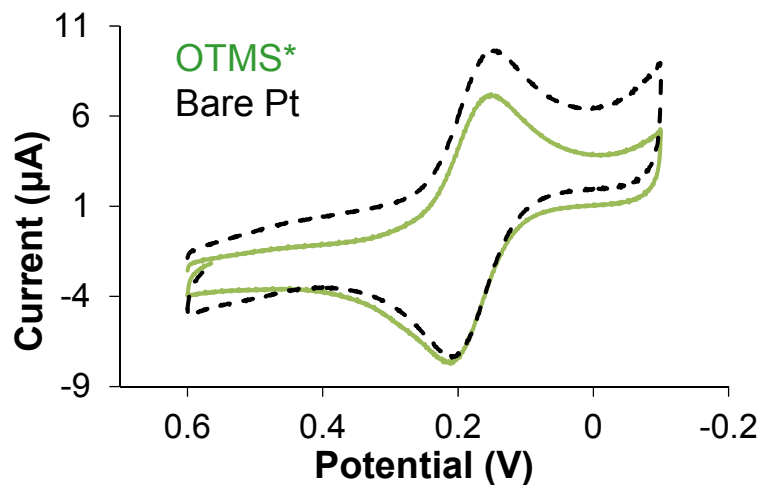
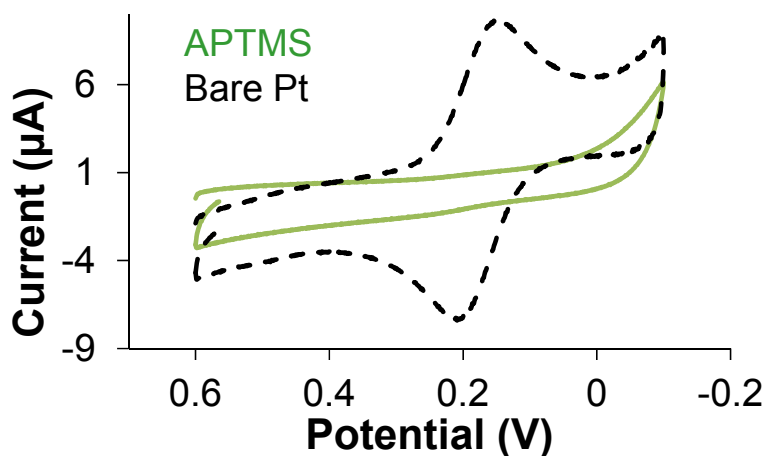
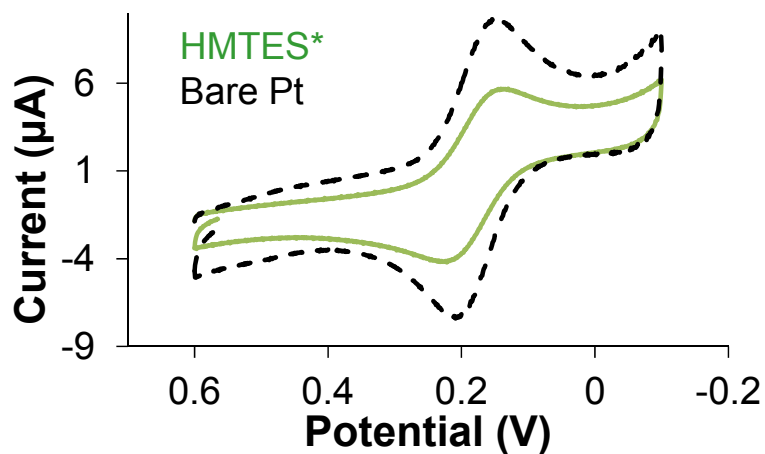


Figure SI-16. Cyclic voltammetry of neutral 1 mM HMFC in 0.1 M HClO_4 at platinum electrodes modified with xerogels formed from different silanes (*green; solid trace*) versus at a bare platinum electrode (*black; dashed*) including **HMTES**, **APTMS**, and **OTMS**. HMFC voltammetry was recorded at 25 mV/sec. Note: *Systems exhibiting the best glucose sensing responses.